



SELECTIVE SHUNT ACTIVE POWER COMPENSATION TECHNIQUES FOR POWER QUALITY ENHANCEMENT

M.Sahithullah
Research Scholar,
Sathyabama University, Chennai

Dr.A.Senthil Kumar
Professor / EEE Dept
Velammal Engineering College

Abstract— This paper propose an optimized compensation algorithm based on linear matrix inequalities in shunt active power filter to eliminate the inefficient power terms under the power rate is limited conditions. Using the IEEE standard 1459 our proposed algorithm recognize the different kinds of in-efficient power terms like active, reactive, unbalanced, harmonics...etc involved by 3-phase four wire system. After that, our algorithm provides a solution by estimate the optimized reference current for SAPF to eliminate the previously selected inefficient power terms. For this reason, the algorithm provides an optimized cost index of different kinds of weighting coefficient. Our proposal has been implemented using a feed forward controller which provides a constant commutation frequency of the SAPF. Simulation results are carried out using MATLAB / SIMULINK and the performance of the proposed scheme is evaluated and compared with the previous methods.

Keywords — Active power filter, IEEE Std. 1459, linear matrix inequality (LMI) algorithm, selective compensation

I. INTRODUCTION

Shunt active power filters (SAPFs) have traditionally been used to improve the quality of the electric systems, reducing the effects of reactive, unbalanced, and harmonic distortion phenomena produced by non efficient loads. To that effect, the SAPF analyzes the grid and generates the non efficient currents demanded by those systems connected downstream of its point of common coupling (PCC). In this way, the transport and distribution networks only have to deliver useful power, thus improving the quality and efficiency of the electric system. The continuous development of the SAPF technology has favored the emergence of various non efficient compensation strategies [1], [2] based each on a different electric power theory. Similarly, multiple current control techniques [3]–[8] and grid synchronization methods [9], [10] have been developed in the last years. Focusing on the compensation strategies, active filters are typically addressed as global filters [2], [6], [11], [12] where the nominal power of the system is large enough so as to compensate all the non efficient phenomena (reactive, unbalance, and harmonic distortion) caused by the surrounding. However, when the non efficient powers of the load vary

significantly (due to load expansions or the simultaneous operation of loads), it may be difficult to preview the size of the SAPF to compensate simultaneously all the potential nonefficient powers. In this context, it is more convenient to compensate separately the different nonefficient phenomena or even a combination of them.

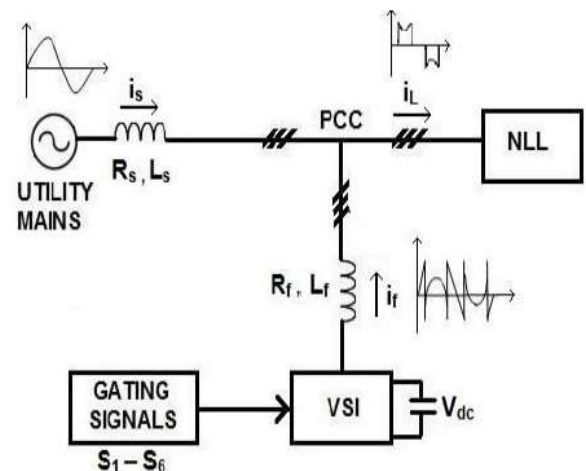


Fig.1. Compensation principle of SAPF

Thus, some authors propose in [4] a selective compensation of harmonic load currents using a set of PI controllers tuned at each of the frequencies of the harmonics to be eliminated. A different approach is presented in [8] where the authors also propose a selective compensation of harmonics with a control technique which they call “selective harmonic compensation.” Both approaches in [4] and [8] do not face either the reactive or the unbalance compensation, and as the number of harmonics to be compensated increases, the proposal in [4] may prove unviable. One step beyond, other authors propose in [13] a selective compensation strategy which does include all nonefficient phenomena. This technique is based on the compensation theory defined in [1], and it uses a neural network to calculate the reference currents. The same authors propose in [14] an algorithm that assigns priority to the compensation of harmonics in front of other nonefficient phenomena when the filter presents



current limitations.

Nonetheless, it does not allow to perfectly profit all the nominal power of the filter. Furthermore, the authors use in both [13] and [14] a hysteresis band regulator to manage the compensation currents. This means that the switching frequency of the converter is dependent on the load parameters and on the grid voltage [15], causing, in this way, an uncontrolled harmonic distortion in the filter output current. On another level, other authors present in [16] a selective compensation using the IEEE Std. 1459 [17] to identify each of the non efficient power terms to be compensated.

The authors use in that work a proportional current regulator and an SVPWM modulation, keeping constant, in that way, the switching frequency of the filter. Also, in [18], the same authors propose another selective compensation strategy, but in this case, they generate the compensation current references using the method of the equivalent conductance. Both strategies proposed in [16] and [18] perform an individual or a combined compensation of the non efficient powers, but none of them take into account the limitations of power that the filter can experience during compensation. This paper proposes an optimization algorithm based on linear matrix inequalities (LMIs) which, using the IEEE Std. 1459 to identify the different power terms, enables a selective compensation of the various non efficient powers existing in the grid without exceeding the nominal power of the SAPF. Moreover, this paper presents a proportional feed forward current regulator designed to control the selected and defined compensation currents while keeping constant the switching frequency of SAPF.

This paper is organized as follows. Section II introduces the theoretical foundations of the algorithm used to analyze non efficient phenomena. In Section III, the reference current generation using the LMI strategy is described. Then, the SAPF characteristics and the controller design are presented in Section IV. Section V is devoted to presenting some compensation results. Finally, some conclusions are stated in Section VI.

II. THEORETICAL BASIS FOR THE GENERATION OF THE COMPENSATION CURRENTS

A. Breakdown of Power Terms According to IEEE Std. 1459

The correct identification of the different power terms forming the apparent power flowing through a line is the basis to perform an optimal compensation of the non efficient powers. The IEEE Std. 1459 defines the effective apparent power (S_e), where V_{e1} and I_{e1} are the fundamental components of the effective voltage and current and V_{eH} and I_{eH} are the non

fundamental components of the effective voltage and current, respectively. Thus, according to it, S_e includes all the power terms concerning efficient and non efficient phenomena that could be required by a generic three-phase load.

$$S_e^2 = (3V_{e1} I_{e1})^2 + (3V_{e1} I_{eH})^2 + (3V_{eH} I_{e1})^2 + (3V_{eH} I_{eH})^2$$

The first term belongs to the fundamental effective apparent Power (S_{e1}), defined as in (1), while the other terms belong to the non fundamental effective apparent power (S_{eN}).

$$S_{e1}^2 = (3V_{e1} I_{e1})^2 \quad (1)$$

$$S_{eN}^2 = (3V_{e1} I_{eH})^2 + (3V_{eH} I_{e1})^2 + (3V_{eH} I_{eH})^2 \quad (2)$$

$$S_e^2 = S_{e1}^2 + S_{eN}^2 \quad (3)$$

Dealing with S_{e1} , it can be divided according to (4) by using the Fortescue transformation. Therefore, it is formed by its positive-sequence component (S_1^+) and a second component including not only the negative and the zero sequences but also the crossed products of the fundamental currents and voltages of any sequence, (S_{U1}). The latter is usually associated to the unbalance of the system and is called unbalance power

$$S_{e1}^2 = (S_1^+)^2 + (S_{U1})^2 \quad (4)$$

In the same way, the term (S_1^+) contains another two terms: a phase and a quadrature one, as shown in (5). These correspond to the fundamental positive-sequence active power (P_1^+), which represents the transference of the actual useful energy, and to the fundamental positive-sequence reactive power (Q_1^+), which represents the bidirectional energy flow due to the phase shift between voltages and currents

$$(S_1^+)^2 = (P_1^+)^2 + (Q_1^+)^2 \quad (5)$$

Moreover, some authors propose the decomposition of S_{U1} into three different terms [19]. In order to derive these new terms, V_{e1} and I_{e1} , both introduced in (1), are divided according to (6) and (7), respectively,

$$V_{e1}^2 = (V_1^+)^2 + (V_{U1})^2 \quad (6)$$

$$I_{e1}^2 = (I_1^+)^2 + (I_{U1})^2 \quad (7)$$

where V_1^+ and I_1^+ are the fundamental positive-sequence voltage and current and V_{U1} and I_{U1} are the fundamental unbalance voltage and current, respectively. From (4) and



taking into account that (S_1^+) can be expressed by the product of V_1^+ and I_1^+ , (8) is deduced

$$(S_{U1})^2 = S_{e1}^2 - (3 V_1^+ I_1^+)^2 \quad (8)$$

$$(S_{U1})^2 = S_{e1}^2 - 9 (V_{e1}^2 - V_{U1}^2) (I_{e1}^2 - I_{U1}^2) \quad (9)$$

$$(S_{U1})^2 = (3V_{e1} I_{e1})^2 + (3V_{U1} I_{U1})^2 - (3V_{U1} I_{U1})^2 \quad (10)$$

The aforementioned terms can be expressed by means of their symmetrical components. Hence, by using the Fortescue transformation, I_{e1} is formed by the currents in

$$I_{e1}^2 = (I_1^+)^2 + (I_1^-)^2 + 4 (I_1^0)^2 \quad (11)$$

where I_1^- and I_1^0 are the fundamental negative- and zero sequence components of current. On the other hand, using (7) and (11), the currents included in I_{U1} are defined in

$$(I_{U1})^2 = (I_1^-)^2 + 4 (I_1^0)^2 \quad (12)$$

Regarding the non fundamental effective apparent power (S_{eN}), it is also divided into three terms: the current distortion effective power (D_{eI}), the voltage distortion effective power (D_{eV}), and the harmonic effective apparent power (S_{eH}). These are defined in (13)–(15), respectively,

$$D_{eI} = 3 V_{e1} I_{eH} \quad (13)$$

$$D_{eV} = 3 V_{eH} I_{e1} \quad (14)$$

$$S_{eH} = 3 V_{eH} I_{eH} \quad (15)$$

Thereupon, S_{eN} quantifies the harmonic effective power Consumed by the loads, which can be also quantified by

$$T H D_{eI} = \frac{I_{eH}}{I_{e1}} \quad (16)$$

The selective compensation developed in this paper intends to cancel the different non efficient power terms (Q_1^+ , S_{u1} , and S_{eN}) separately or even a combination of them.

III. REFERENCE CURRENT GENERATION

The generation of reference currents to introduce in the SAPF is determined by the magnitude of the various non efficient powers that would be desirable to cancel but is also limited by the nominal power of the SAPF itself. Measuring the load currents and using the power definitions provided by the IEEE Std. 1459, the reference currents are calculated so as to selectively compensate the different non efficient phenomena without exceeding the maximum rated current of

the SAPF. To do this, a cost index to be minimized is formulated. This index contains all the power terms to be compensated and assigns a relative weight to each of them. It also takes into account the power limitation of SAPF. For the proper calculation of this index, it is necessary to correctly identify the grid, the load, and the SAPF phase currents.

In this sense, defines each of the SAPF phase currents ($k = a, b, c$) in rectangular coordinates, where the subscripts r and i denote the real and the imaginary part, respectively

$$\bar{I}_{k1 \text{ SAPF}} = I_{k1r \text{ SAPF}} + j I_{k1i \text{ SAPF}} \quad (17)$$

On the other hand, (24) defines the rms value of the SAPF phase currents

$$I_{k \text{ SAPF}}^2 = I_{k1 \text{ SAPF}}^2 + I_{kH \text{ SAPF}}^2 \quad (18)$$

where $I_{k \text{ SAPF}}$ is the rms value of the total current for each of the SAPF phases and $I_{kH \text{ SAPF}}$ is the rms value of the total harmonic content existing in those phase currents.

In the same way, (19)–(22) define the fundamental and the rms currents for both load and grid phases, respectively

$$\bar{I}_{k1 \text{ load}} = I_{k1r \text{ load}} + j I_{k1i \text{ load}} \quad (19)$$

$$I_{k \text{ load}}^2 = I_{k1 \text{ load}}^2 + I_{kH \text{ load}}^2 \quad (20)$$

$$\bar{I}_{k1s} = I_{k1rs} + j I_{k1is} \quad (21)$$

$$I_{ks}^2 = I_{k1s}^2 + I_{kHs}^2 \quad (22)$$

Finally, it is to be noted that, provided that all the harmonic currents have been included within a single term, it makes no sense to operate with current phasors and it is preferable to use the rms values instead.

A. Constraints

Once the different phase currents have been defined, the constraints of the problem have to be set. In this paper, the main constraint introduced is associated to the limitation in the rms total phase-current value defined for the SAPF, i.e.

$$I_{k \text{ SAPF}} \leq I_{\text{max}} \quad (23)$$

where I_{max} is usually defined as the rms SAPF nominal current. This inequality can also be rewritten as in



$$I_{k1r\text{ SAPF}} + I_{k1i\text{ SAPF}} + I_{k1H\text{ SAPF}} \leq I_{\max} \quad (24)$$

B. Unbalances in the Fundamental Component

The obtainment of the positive-, negative-, and zero- sequence grid current components requires the use of the Fortescue transformation. As described in Section II-A, the use of these components allows defining the term S_{U1} , defined in (14), that minimizes the power term associated to unbalances. In case compensating it was the unique goal of the SAPF, the reference currents could be calculated, using the measured load currents and grid voltages, according to

$$\begin{aligned} & \text{Min } (S_{U1})^2 \quad \text{subject to} \\ & I_{k1r\text{ SAPF}} + I_{k1i\text{ SAPF}} + I_{k1H\text{ SAPF}} \leq I_{\max} \\ & \bar{I}_{k1\text{load}} = \bar{I}_{k1\text{SAPF}} + \bar{I}_{k1} \end{aligned} \quad (25)$$

where $a = e^{(2\pi/3)\mathbf{j}}$. One can observe how this problem contains complex variables and quadratic constraints that require some treatment to become a resolvable LMI problem using the tools introduced in Section II-B. This transformation is detailed in the coming sections.

C. Fundamental and Positive-Sequence Reactive Power

To improve the power factor of the system, the fundamental and positive-sequence reactive power can be calculated as in

$$Q_1^+ = 3 \text{Im} (V_1^+ (I_1^+)^*) \quad (26)$$

Therefore, if the unique goal of the SAPF was, in this case, to minimize this power, Q_+ , a new optimization problem that used the same constraints as that in, could be defined, but this would incorporate $(Q_+)^2$ as the cost index instead.

D. Apparent Power Due to Current Harmonics

The current harmonic evaluation is global, i.e., without distinguishing the harmonic order, as defined in the IEEE Std. 1459. Therefore, taking again into account the current signs defined in at the PCC, (29) can be written

$$i_{kH\text{load}}(t) = i_{kH\text{SAPF}}(t) + i_{kH\text{s}}(t) \quad (27)$$

To the same extent, (30) defines the value of the harmonics introduced by the SAPF as a ratio of the load harmonics

$$i_{kH\text{SAPF}}(t) = \alpha i_{kH\text{load}}(t) \quad (28)$$

where α is a variable defined between 0 and 1 which will determine the harmonic compensation level for each of the phases. In this way, it can be guaranteed that the effective harmonic current value will be as in

$$I_{eH\text{SAPF}} = \alpha I_{eH\text{load}} \quad (29)$$

Therefore, due to the scalar nature of the α coefficient, the definition in (31) can be granted

$$I_{eH\text{s}} = (1 - \alpha) I_{eH\text{load}} \quad (30)$$

Moreover, according to (32), the S_{eN} terms defined in can be reformulated as in

$$D_{eI} = 3 V_{eI} I_{eH\text{load}} (1 - \alpha) \quad (31)$$

$$D_{eV} = 3 V_{eH} I_{eI\text{s}} \quad (32)$$

$$S_{eH} = 3 V_{eH} I_{eH\text{load}} (1 - \alpha) \quad (33)$$

Note from these equations that the D_{eV} straightly depends on the fundamental grid current component and on the grid voltage harmonics. Given that the SAPF controls its currents and, consequently, the grid currents, the only way to limit this non efficient power term is to reduce the fundamental grid current component. In this way, because the grid voltage is independent of the system, the optimization performed in this work does not take into account this term.

E. Active Power Delivered by the SAPF

Finally, the SAPF could also control the active power exchanged with the grid. This power is set to a null value if the dc bus of the SAPF is formed by capacitors, given that any active power exchange would modify the bus voltage dramatically. Conversely, if the dc bus is formed by an energy storage system presenting a significant energy capacity (batteries, super-caps, etc.), some control strategies can be implemented in the SAPF to also manage the fundamental active power exchanges ($P_{\text{ref SAPF}}$). This power can be written as a function of the

$$P_{k1\text{SAPF}} = \text{Re} (V_{k1\text{s}} I_{k1\text{SAPF}}^*) \quad (34)$$

$$P_{a1\text{SAPF}} + P_{b1\text{SAPF}} + P_{c1\text{SAPF}} = P_{\text{ref SAPF}} \quad (35)$$

where $V_{k1\text{s}}$ is the fundamental voltage for each of the grid phases.



IV. DESCRIPTION OF THE SYSTEM

A. SAPF

The proposal presented in this paper has been tested in a system such as the one represented in Fig. 3, where the SAPF is connected at the PCC with the low voltage grid and some local loads. As can be observed, the SAPF is formed by a three legged split-capacitor inverter and a three-phase output filter (with values $R_a = R_b = R_c = 0.4 \Omega$ and $L_a = L_b = L_c = 6 \text{ mH}$). Regarding the load, used in both the simulations and the laboratory tests, this contains a linear unbalanced three-phase load in parallel to a nonlinear balanced load. The former is constituted by resistances and windings (with values $R_{load} = 32 \Omega$, $L_{load} = 18 \text{ mH}$, $R_{bload} = 50 \Omega$, $L_{bload} = 9 \text{ mH}$, and $R_{cload} = 100 \Omega$), and the latter is constituted by three onephase noncontrolled rectifiers feeding an RC load through an inductive filter (with values $L = 5 \text{ mH}$, $C = 2200 \mu\text{F}$, and $R = 100 \Omega$).

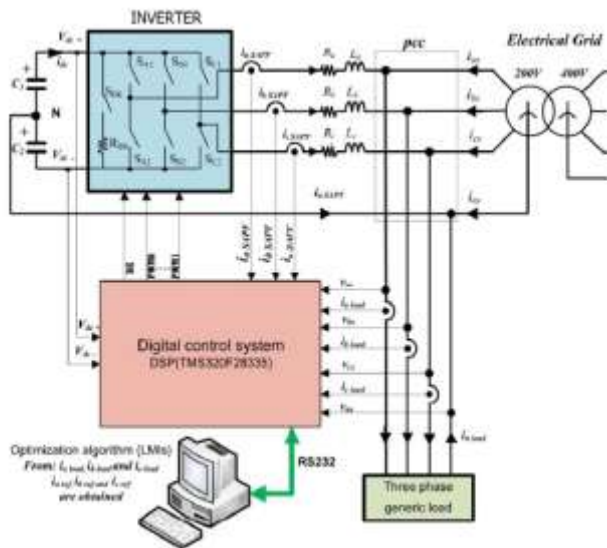


Fig.2. connection of the complete experimental system

The capacitance of the dc bus is $C1 = C2 = 5.44 \text{ mF}$, and the operating voltage is 550 V. Its midpoint is connected to the grid neutral to allow the circulation of the zero-sequence currents. To protect the dc bus against overvoltage, the SBK IGBT transistor and external RBK are used. The control of the dc bus voltage implements a regulator such as that proposed in [16] and [18]. A 400/200-V wye-wye transformer connects the SAPF and the three-phase loads to the grid in order to get a good modulation gain from the 550 V of the dc bus. The switching frequency is 27.15 kHz, which is also the sampling frequency implemented for the control and the acquisition of currents and voltages. In this way, the load current is sampled 543 times every grid cycle.

Thereupon, once a second, the DSP driving the SAPF sends the last-cycle load currents via a RS232 communication to a PC. This calculates the updated current references and returns them to the DSP, which generates the SAPF modulation according to them. Thus, an external PC is the one running the optimization algorithm. With this approach, it is guaranteed that the SAPF will not exceed its nominal power. On the other hand, when a load current transient occurs, the compensation currents are not adequate, for 1 s, as the new references are still being calculated on the PC.

B. Current Controller

A current regulator quick enough to correctly track the current references and thus properly perform the non efficient phenomenon compensation has been designed and implemented. This proposed regulator is a proportional (P) feed forward controller such as the one described. It is formed by two terms: a standard P regulator (which generates a control action proportional to the tracking error) and a feed forward term, which inverts the system dynamics.

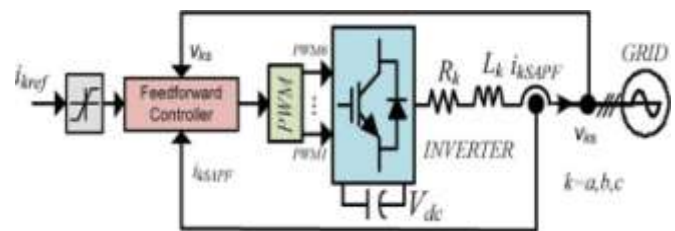


Fig.3. Block diagram of current control implemented in SAPF

To do this inversion, the grid voltage and current reference are needed. This way, in an ideal situation with no disturbances, the second term calculates the voltages needed to get the desired reference current from the SAPF.

This control structure allows an improved dynamic response from a standard P regulator in systems, such as the one describe here, where the feed forward term only needs to calculate derivatives of a reference signal (and not a measurement). Usual problems in feed forward controllers arising from the fact of differentiating noisy measured signals are, in this way, avoided. Also, note that a saturation block has been added in order to limit the maximum pointwise value of the reference current. This way, references higher than the peak current of the IGBT transistors are never demanded. To design the feed forward regulator (see Fig. 5), the SAPF output current and voltages are formulated as in

$$V_{k \text{ SAPF}} = R_k i_{k \text{ ref}} + L_k \frac{d}{dt} i_{k \text{ ref}} + V_{ks} + P (i_{k \text{ ref}} - i_{k \text{ SAPF}}) \quad (36)$$

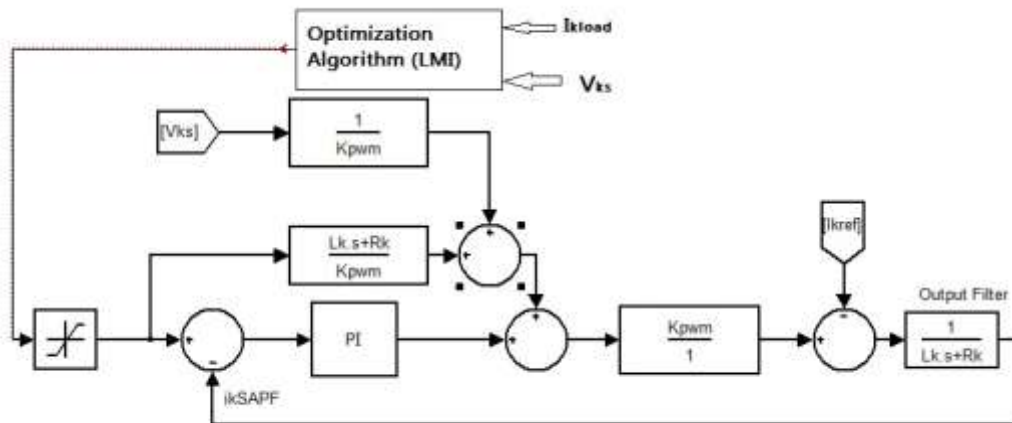


Fig.4 Block diagram of the feed forward current regulator

Where v_k SAPF is the converter output voltage, v_{ks} is the grid voltage, and R_k and L_k are the values of the SAPF output filter impedance of each phase. Then, the P regulator is defined by forcing the settling time to $t_{st} = 2$ ms and $k_{PWM} = 1$, using the characteristic. In this way, a proportional gain such as that in is obtained.

$$1 + P G_{OL}(s) = 1 + P * K_{PWM} \frac{1}{R_k + L_k s} = 0 \quad (37)$$

The below figure shows the Block diagram of the feed forward current regulator.

V. OBTAINED RESULTS

Simulations tests have been carried out to analyze the performance of the proposed optimization algorithm. Simulations used a digital model developed in Matlab / Simulink and its SimPowerSystem toolbox. For such a scenario, the performance of the SAPF under different operation conditions has been analyzed. The analysis focuses on the evaluation with Mathcad of the different power terms associated to each of the corresponding non efficient phenomena described by the IEEE Std. 1459. The evaluation is performed both before and after activating the compensation, using the voltages and currents measured at the PCC. The study cases ranged from a global compensation of the non efficient phenomena to different selective compensations that prioritized the various non efficient power terms. Finally, the performance of the proposed optimization algorithm is compared to a similar approach from the literature. Figs. 6 show the simulated and experimental results, respectively, obtained during the connection transient of this global compensation.

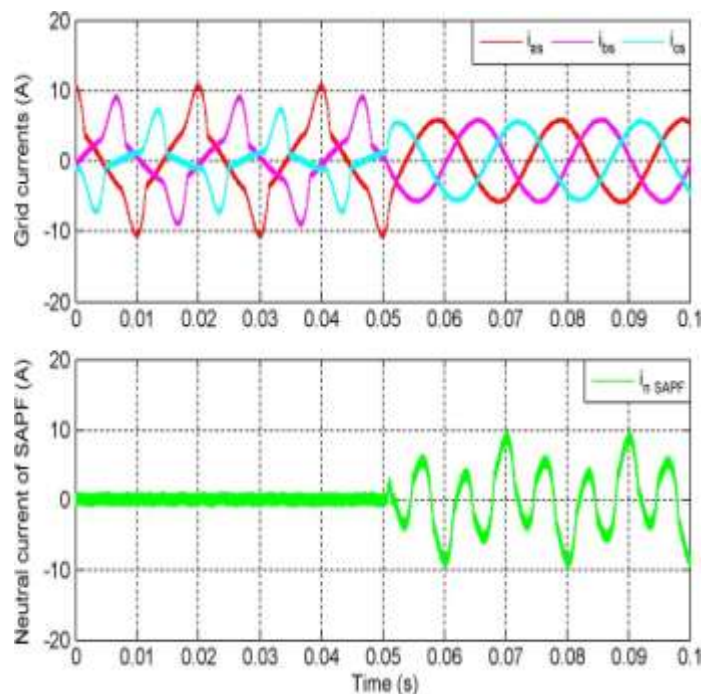


Fig.5. Grid and SAPF neutral current transient during the connection of the SAPF for a global compensation

TABLE I
POWER TERMS WHEN THE SAPF HAS NO POWER CONSTRAINTS

BEFORE ANY KIND OF COMPENSATION			
$S_{U1}=556.46$ VA	$Q_1^+=308.64$ var	$S_{eN}=1007.42$ VA	$THD_{eI}=0.65$
AFTER THE GLOBAL COMPENSATION			



$S_{UI}=64.43$ VA	$Q_1^+=14.40$ var	$S_{eN}=209.35$ VA	$THD_{ef}=0.14$
----------------------	----------------------	-----------------------	-----------------

Finally, the presented algorithm is compared with that proposed in [14], which also enables a SAPF to perform a selective compensation of the non efficient phenomena. In that work, the authors introduce a priority-based compensation, where the first preference is given to the harmonics. From there on, if the SAPF is still powerful enough, the authors propose to reduce the negative-sequence current, associated to unbalance, down to 5% of the full load current. Then, they propose to compensate the reactive power until a power factor of 0.85 is achieved. Finally, if the SAPF still has some capacity left at this point, both unbalance and reactive power are compensated with weightages in the ratio of 4 : 1. This proposal mainly differs from the algorithm presented here in two aspects: First, the priority of compensation in [14] is assigned on the basis of the considered gravity of the non efficient effects, calculated from the SRF current decomposition, while in the cost index proposed here in Section III-F, based on the IEEE Std. 1459 power terms, the weighting factors can be freely modified; second, [14] limits the algebraic sum of the current components, instead of the sum of squares as in (30). In this way, while this approach guarantees that the SAPF currents do not exceed the filter limitations, in a general case, these currents will stay far from the real rms filter limit, wasting some of its compensation capacity.

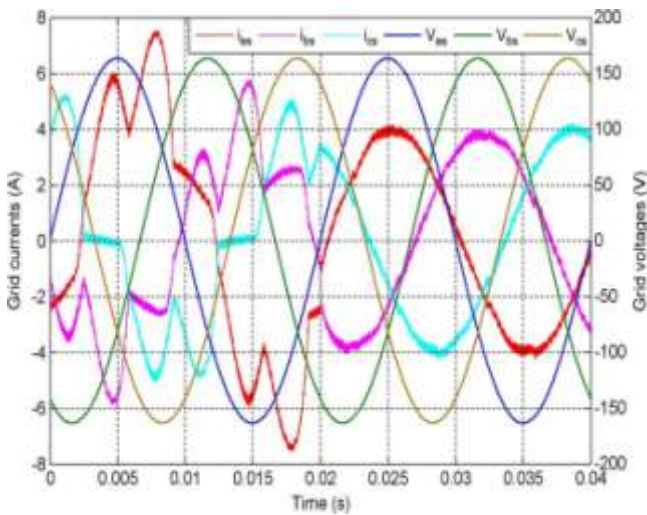


Fig.6. Grid currents after compensation with the algorithm from [14]

To illustrate this point, a new simulation case comparing both algorithms is developed (note that the load conditions of the previous cases cannot be replicated with the algorithm from [14] because of the absence of a neutral wire in their approach). In this case, the load contains a linear unbalanced three-phase load in parallel to a nonlinear balanced load. The former is constituted by resistances and windings (with values $L_{load} = 230$ mH, $L_{load} = 100$ mH, and $R_{load} = 1000 \Omega$), and the

latter is constituted by a three-phase noncontrolled rectifier feeding an RC load through an inductive filter (with values $L = 5$

mH, $C = 2200 \mu\text{F}$, and $R = 75 \Omega$). The SAPF's current limit is set in this case to 2.5 A.

In order to get a similar behavior in terms of the relative importance given to the different nonefficient phenomena from the LMI algorithm to the proposal in [14], the weighting coefficients are set to $K_U = 500$, $K_Q = 1$, and $K_H = 1000$. Fig. 6 and Fig.7 Show the results obtained with each algorithm. It can be seen how both approaches, as expected, almost completely eliminate the harmonic currents.

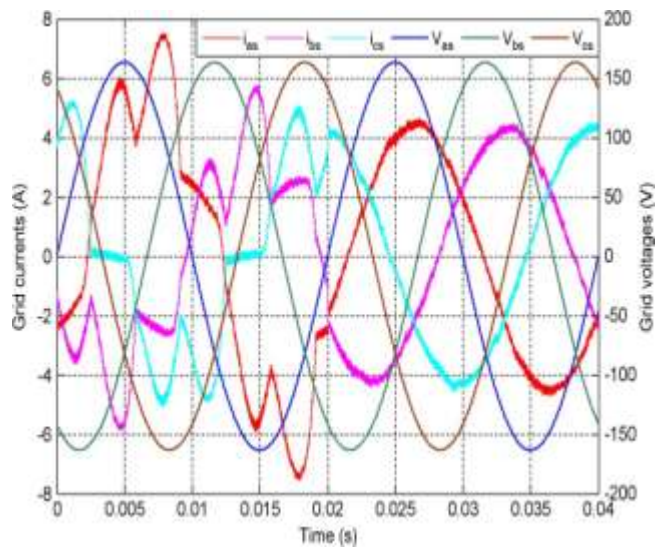


Fig.7. Grid currents after compensation with the LMI algorithm

TABLE III
POWER TERMS OF THE GRID CURRENTS

Before Any Kind Of Compensation			
$S_{UI}=374.45$ VA	$Q_1^+=316.64$ var	$S_{eN}=355.42$ VA	$THD_{ef}=0.295$
After compensation with Algorithm Proposed in [14]			
$S_{UI}=33.43$ VA	$Q_1^+=450.40$ var	$S_{eN}=46.35$ VA	$THD_{ef}=0.037$
After The Compensation With LMI Algorithm			
$S_{UI}=6.43$ VA	$Q_1^+=114.40$ var	$S_{eN}=44.35$ VA	$THD_{ef}=0.039$

VI. CONCLUSION

The proposed optimized compensation algorithm provides a rated power of SAPF to grid for compensating the in-efficient power factors of grid. This proposed algorithm is based on



LMIs, which estimate the SAPF compensation current to eliminate its rated power. Simulation results show the performance of SAPF during a selective compensation was improved compare with other proposed works and it achieves a 0.65% higher reduction in S_{eN} , a 7.15% higher reduction in SU 1, and a 54.3% higher reduction in $Q+$.

VII. REFERENCES

- [1] H. Akagi, E. Watanabe, and M. Aredes, "More power to you (review of Instantaneous Power Theory and Applications to Power Conditioning by Akagi, H. et al.; 2007) [book review]," *IEEE Power Energy Mag.*, vol. 6, no. 1, pp. 80–81, Jan./Feb. 2008.
- [2] S. Orts *et al.*, "Achieving maximum efficiency in three-phase systems with a shunt active power compensator based on IEEE Std. 1459," *IEEE Trans. Power Del.*, vol. 23, no. 2, pp. 812–822, Apr. 2008.
- [3] M. Angulo, D. A. Ruiz-Caballero, J. Lago, M. L. Heldwein, and S. A. Mussa, "Active power filter control strategy with implicit closed-loop current control and resonant controller," *IEEE Trans. Ind. Electron.*, vol. 60, no. 7, pp. 2721–2730, Jul. 2013.
- [4] F. Briz, P. Garcia, M. W. Degner, D. Diaz-Reigosa, and J. M. Guerrero, "Dynamic behavior of current controllers for selective harmonic compensation in three-phase active power filters," *IEEE Trans. Ind. Appl.*, vol. 49, no. 3, pp. 1411–1420, May/Jun. 2013.
- [5] J. He, Y. W. Li, and F. Blaabjerg, "Flexible microgrid power quality enhancement using adaptive hybrid voltage and current controller," *IEEE Trans. Ind. Electron.*, vol. 61, no. 6, pp. 2784–2794, Jun. 2014.
- [6] S. Orts-Grau *et al.*, "Improved shunt active power compensator for IEEE Standard 1459 compliance," *IEEE Trans. Power Del.*, vol. 25, no. 4, pp. 2692–2701, Oct. 2010.
- [7] Q.-N. Trinh and H.-H. Lee, "An advanced current control strategy for three-phase shunt active power filters," *IEEE Trans. Ind. Electron.*, vol. 60, no. 12, pp. 5400–5410, Dec. 2013.
- [8] H. Zhou *et al.*, "Selective harmonic compensation (SHC) PWM for grid-interfacing high-power converters," *IEEE Trans. Power Electron.*, vol. 29, no. 3, pp. 1118–1127, Mar. 2014.
- [9] J. C. Alfonso-Gil, J. J. Vague-Cardona, S. Orts-Grau, F. J. Gimeno-Sales, and S. Segui-Chilet, "Enhanced grid fundamental positive-sequence digital synchronization structure," *IEEE Trans. Power Del.*, vol. 28, no. 1, pp. 226–234, Jan. 2013.
- [10] F. Gonzalez-Espin, E. Figueres, and G. Garcera, "An adaptive synchronous-reference-frame phase-locked loop for power quality improvement in a polluted utility grid," *IEEE Trans. Ind. Electron.*, vol. 59, no. 6, pp. 2718–2731, Jun. 2012.
- [11] A. Bhattacharya and C. Chakraborty, "A shunt active power filter with enhanced performance using ANN-based predictive and adaptive controllers," *IEEE Trans. Ind. Electron.*, vol. 58, no. 2, pp. 421–428, Feb. 2011.
- [12] P. Acuna, L. Moran, M. Rivera, J. Dixon, and J. Rodriguez, "Improved active power filter performance for renewable power generation systems," *IEEE Trans. Power Electron.*, vol. 29, no. 2, pp. 687–694, Feb. 2014.
- [13] B. Singh, V. Verma, and J. Solanki, "Neural network-based selective compensation of current quality problems in distribution system," *IEEE Trans. Ind. Electron.*, vol. 54, no. 1, pp. 53–60, Feb. 2007.
- [14] B. Singh and V. Verma, "Selective compensation of power-quality problems through active power filter by current decomposition," *IEEE Trans. Power Del.*, vol. 23, no. 2, pp. 792–799, Apr. 2008.
- [15] R. Gupta, "Generalized frequency domain formulation of the switching frequency for hysteresis current controlled VSI used for load compensation," *IEEE Trans. Power Electron.*, vol. 27, no. 5, pp. 2526–2535, May 2012.